The Astrophysical Journal Letters, 984:L66 (7pp), 2025 May 10 https://doi.org/10.3847/2041-8213/adcee3

On the Evidence of a Dark Matter Density Spike around the Primary Black Hole in OJ 287

Debabrata Deb[1], Achamveedu Gopakumar[2], and Mauri J. Valtonen[3,4]
[1] The Institute of Mathematical Sciences, C.I.T. Campus, Taramani, Chennai 600113, India; d.deb32@gmail.com
[2] Department of Astronomy and Astrophysics, Tata Institute of Fundamental Research, Mumbai 400005, India
[3] FINCA, University of Turku, FI-20014 Turku, Finland
[4] Tuorla Observatory, Department of Physics and Astronomy, University of Turku, FI-20014 Turku, Finland
Received 2025 February 8; revised 2025 April 1; accepted 2025 April 7; published 2025 May 8

Abstract

The central engine of blazar OJ 287 is arguably the most notable supermassive black hole (SMBH) binary candidate that emits nanohertz (nHz) gravitational waves. This inference is mainly due to our ability to predict and successfully monitor certain quasiperiodic doubly peaked high brightness flares with a period of ∼12 yr from this blazer. The use of post-Newtonian accurate SMBH binary orbital description that includes the effects of higher-order gravitational-wave emission turned out to be a crucial ingredient for accurately predicting the epochs of such Bremsstrahlung flares in our SMBH binary central engine description for OJ 287. It was very recently argued that one should include the effects of dynamical friction, induced by certain dark matter density spikes around the primary SMBH, to explain the *observed* decay of SMBH binary orbit in OJ 287. Invoking binary pulsar timing-based arguments, measurements, and OJ 287's orbital description, we show that observationally relevant SMBH binary orbital dynamics in OJ 287 are insensitive to dark-matter-induced dynamical friction effects. This implies that we could only provide an upper bound on the spike index parameter rather than obtaining an observationally derived value, as argued by M. H. Chan and C. M. Lee.

Unified Astronomy Thesaurus concepts: BL Lacertae objects (158); Black hole physics (159); Dark matter density (354); Dark matter distribution (356)

1. Introduction

Individual supermassive black hole (SMBH) binaries with milliparsec orbital separations are promising nanohertz (nHz) gravitational-wave (GW) sources for the rapidly maturing pulsar timing array (PTA) efforts (T. Liu et al. 2023). These PTA efforts include those by the International Pulsar Timing Array consortium (IPTA; M. Falxa et al. 2023; G. Agazie et al. 2024) and its constituents, namely, the European PTA (EPTA; G. Desvignes et al. 2016; EPTA Collaboration et al. 2023a), the Indian PTA (InPTA; B. C. Joshi et al. 2018; P. Tarafdar et al. 2022), the North American Nanohertz Observatory for Gravitational Waves (NANOGrav; G. Agazie et al. 2023a, 2023b), the Australia-based Parkes PTA (PPTA; R. N. Manchester et al. 2013; A. Zic et al. 2023), and MeerKAT PTA (M. T. Miles et al. 2023). The constituent PTAs of IPTA, namely, NANOGrav, EPTA+InPTA, PPTA, and the Chinese PTA in 2023, reported certain compelling evidence for the presence of a stochastic GW background (GWB) in nHz frequencies in their respective data sets (G. Agazie et al. 2023b; EPTA Collaboration et al. 2023b; D. J. Reardon et al. 2023; H. Xu et al. 2023).

It is expected that such a GWB could be due to inspiral nHz GWs from an ensemble of SMBH binaries though there are other possible exotic explanations (A. Afzal et al. 2023; EPTA Collaboration et al. 2024a). Additionally, recent NANOGrav and EPTA+InPTA investigations point toward tentative evidence for GWs from individual SMBH binaries in their latest data sets (G. Agazie et al. 2023c; EPTA Collaboration et al. 2024b). It is expected that such binaries should allow the IPTA consortium to pursue persistent multimessenger nHz GW astronomy, especially during the era of Square Kilometre Array and Deep Synoptic Array-2000 (Y. Wang & S. D. Mohanty 2017; G. Hallinan et al. 2019; B. C. Joshi et al. 2022; H. Padmanabhan & A. Loeb 2023). It may be noted that SMBH binaries naturally arise from the hierarchical structure formation scenario that involves galaxy mergers (C. M. Baugh 2006). Initially, there was a lot of uncertainty about the subsequent evolution of SMBH binaries, especially about their ability to reach the GW-driven inspiral phase. However, with later work, both analytical and computer simulations, it has become clear that all binaries formed in this way will merge within a few billion years at most (M. C. Begelman et al. 1980; P. J. Armitage & P. Natarajan 2002; G. Kulkarni & A. Loeb 2012; M. Valtonen & H. Karttunen 2006; M. Iwasawa et al. 2011; S. Liao et al. 2024). Unfortunately, electromagnetic observations are only capable of providing potential SMBH binary candidates, and unique blazer OJ 287 and PKS 2131-021 are two promising SMBH binary candidates with milliparsec orbital separations, thanks to decades-long electromagnetic observations (M. J. Valtonen et al. 2021; S. O'Neill et al. 2022)

Thoroughly tested SMBH binary central engine description for OJ 287 is influenced by its century-long light curve, mainly due to the position of this 13 mag active galactic nucleus on the ecliptic (L. Dey et al. 2019). Further, the regular monitoring of OJ 287 in the past decades reveals the presence of quasiperiodic doubly peaked high brightness flares with a deductible period of ∼12 yr. The constituent peaks are separated by a few years, and there exists a longer timescale variation in its apparent magnitude with a period of ∼60 yr (L. Dey et al. 2019). It is possible to explain these observed (and unique) magnitude variations by invoking a central engine

description for OJ 287 that involves an SMBH binary (H. J. Lehto & M. J. Valtonen 1996). This model requires a secondary SMBH that orbits a more massive primary SMBH in a precessing eccentric orbit with a redshifted orbital period of ∼12 yr. The inclined secondary black hole (BH) trajectory ensures that it impacts the accretion disk of the primary twice every orbit leading to the observed bremsstrahlung impact flares (H. J. Lehto & M. J. Valtonen 1996). The use of post-Newtonian (PN) accurate orbital trajectory for the secondary SMBH allowed some of us to predict the starting times of the eventually observed impact flares of 2005, 2007, and 2015 (M. J. Valtonen et al. 2006, 2008, 2016). It may be noted that the PN approximation provides general relativistic corrections to the Newtonian dynamics of an SMBH binary as an expansion in powers of $(v/c)^2 \sim GM/c^2r$, where v, M, and r, respectively, denote the relative velocity, total mass, and the relative separation of the system. For example, the 3PN order provides $(v/c)^6$ order general relativity (GR) corrections to the Newtonian point particle binary dynamics (L. Blanchet 2024). Here c is the speed of light. The most up-to-date SMBH binary central engine description for OJ 287 employs PN-accurate orbital dynamics that incorporate 3PN-accurate conservative orbital dynamics associated with nonspinning SMBH binaries, leading order spin–orbit, spin–spin interactions, and effects of next-to-next-to-next-to quadrupolar-order GW emission (L. Dey et al. 2018).

These considerations allowed us to predict in 2018 that the next impact flare should peak on 2019 July 31, around noon GMT (L. Dey et al. 2018). The detailed analysis of the multiepoch Spitzer observations and the predicted similarities between the 2019 and 2007 impact flare lightcurves allowed us to determine that the expected OJ 287's "Eddington flare" arrived only 90 minutes late, within the 4 hr predicted accuracy (S. Laine et al. 2020). Unfortunately, the retirement of the Spitzer telescope on 2020 January 30 ensured that the predicted 2022 July/August impact flare was not observable like the Eddington flare (L. Dey et al. 2018). However, the closely monitored large-amplitude optical intraday flare on 2021 November 12 could be associated with the jet activities from OJ 287's secondary SMBH (M. J. Valtonen et al. 2024). Due to these multiple successful OJ 287 observational campaigns, launched essentially to verify the predicted occurrences of impact flares, we have the following measurements for its SMBH binary parameters: masses of the primary and secondary SMBH are $\sim 18.35 \times 10^9\, M_\odot$ and $150 \times 10^6\, M_\odot$, respectively, while the primary SMBH Kerr parameter is ∼0.38 and the orbital eccentricity is ∼0.66. Additionally, both the orbital period (redshifted) and its time derivative are derived (or estimated) parameters, as emphasized in Table 2 of L. Dey et al. (2018), and their values are $P_{\rm obs}^{2017} = 12.062 \pm 0.007$ yr and $\dot{P}_{\rm obs} = -(0.00099 \pm 0.00006)$, respectively. Note that the higher-order GW terms decrease the orbital energy loss by ∼5%, and therefore it is important that they are included in the orbit solution (M. J. Valtonen et al. 2018; L. Dey et al. 2018). Interestingly, the deduced rate of orbital period decay is 9 orders of magnitude higher than the observed (measured) rate in PSR 1913+16, as noted in L. Dey et al. (2018).

Therefore, it is surprising to see inferences of M. H. Chan & C. M. Lee (2024) where they argued that the SMBH binary orbital dynamics in OJ 287 are affected by dynamical friction induced by certain dark matter (DM) density spikes around its primary SMBH. This conclusion originates from their argument that certain inequality exists between the measured and estimated values of GW energy luminosity, computed using OJ 287's SMBH binary parameters, listed in Table 2 of L. Dey et al. (2018). Specifically, M. H. Chan & C. M. Lee (2024) showed that their "estimated" energy-loss rate due to GW emission is significantly lower than their "observed" energy-loss rate, with a discrepancy of more than 4.3σ. This prompted them to employ a dark matter density spike around the primary SMBH, invoking the resulting dynamical friction to provide the extra energy-loss rate to account for their inferred discrepancy in OJ 287's observed energy-loss rate. These considerations allowed them to estimate spike index γ_{sp} whose value turned out to agree with its predicted value based on the adiabatically growing SMBH model (P. Gondolo & J. Silk 1999; B. D. Fields et al. 2014).

In what follows, we take a closer look at the arguments of M. H. Chan & C. M. Lee (2024) and demonstrate that their consistency test strictly works for binary systems like PSR 1913+16 where decades-long accurate timing of ∼10,000 times of arrival (ToAs) of radio pulses had provided independent measurements for its orbital period and the first-time derivative (P_b and $\dot{P}_b$). After that, we provide new estimates for OJ 287's orbital period and its derivative that employ measured values of the independent parameters of SMBH binary central engine description as listed in Table 2 of L. Dey et al. (2018). We also clarify why one should not use the "derived" estimates for OJ 287's orbital period and its derivative as listed in Table 2 of L. Dey et al. (2018). With our new estimates for P_b and $\dot{P}_b$, we show that the consistency test of M. H. Chan & C. M. Lee (2024) works for OJ 287 as expected. Interestingly, this test also shows why PN contributions to GW emission are relevant while performing the test. After that, we provide an upper bound for $\gamma_{\rm sp}$ by associating the uncertainties in our estimated GW luminosities, influenced by M. W. Horbatsch & C. P. Burgess (2012).

2. On the Equality between the Estimated and Measured GW Luminosities: The Relevance of Independently Measured Parameters

We begin by taking a closer look at the consistency test that involves the measured and estimated GW luminosities, as detailed in M. H. Chan & C. M. Lee (2024). This test, as noted earlier, was pursued to explore if non-GR effects influence the dynamics of OJ 287's SMBH binary. The test involves computing $\dot{E}_{\rm GW}$, which is the negative of the quadrupolar-order orbital averaged GW luminosity $\langle \mathcal{L} \rangle$ (L. Blanchet & G. Schaefer 1989), as given by Equation (2) of M. H. Chan & C. M. Lee (2024):

$$\dot{E}_{\rm GW} = -\frac{32G^4}{5c^5}\frac{\mu^2 M^3}{a^5(1-e^2)^{7/2}}\left(1 + \frac{73}{24}e^2 + \frac{37}{96}e^4\right), \quad (1)$$

where the reduced mass and total mass of the SMBH binary are given by $\mu = m_1 m_2/M$ and $M = m_1 + m_2$, respectively, and m_1 and m_2 stand for the masses of the primary and secondary black holes, respectively. Here a and e denote the semimajor axis and eccentricity parameter, respectively. G denotes the Newtonian gravitational constant, and c is the speed of light. M. H. Chan & C. M. Lee (2024) evaluated the above expression by employing the measured parameters of OJ 287's SMBH binary model, namely, m_1, m_2, and e, as provided in Table 2 of

L. Dey et al. (2018). However, the value for the orbital semimajor axis a was adopted from M. J. Valtonen & H. J. Lehto (1997), where it was estimated using the redshifted orbital period of 12.07 yr.

In the next step, they obtained the same quantity while using the energy balance argument, which demands that the luminosity of GW emission, namely, $\langle \mathcal{L} \rangle$, should be balanced by a decrease in the Newtonian energy of the compact binary as the rest masses of these compact objects stay constant. The use of Kepler's third law ensures that binary orbital period P_b decreases due to the emission of GWs such that

$$\frac{\dot{P}_b}{P_b} = +\frac{3}{2\,E\,\mu}\,\langle \mathcal{L} \rangle, \tag{2}$$

where $\dot{P}_b$ stands for the time derivative of P_b and E gives the Newtonian orbital binding energy. This leads to Equation (3) of M. H. Chan & C. M. Lee (2024), which reads

$$\dot{E} = -\frac{2E\dot{P}_b}{3P_b}. \tag{3}$$

The consistency test expects numerical estimates for $\dot{E}$ and $\dot{E}_{\rm GW}$ should be identical, provided the parameters that appear on the right-hand side of Equations (1) and (3) are independently measured. Employing various parameters of OJ 287's SMBH binary description, including redshifted orbital period $P_{\rm orb}^{2017}$ and corresponding decay rate $\dot{P}_{\rm orb}$, listed in Table 2 of L. Dey et al. (2018), it was argued that there exists a significant 4.3σ discrepancy between the numerical values of $\dot{E}$ and $\dot{E}_{\rm GW}$ (M. H. Chan & C. M. Lee 2024). These two estimates turned out to be $-(3.66 \pm 0.24) \times 10^{41}$ W for $\dot{E}$ and $-(2.62 \pm 0.02) \times 10^{41}$ W for $\dot{E}_{\rm GW}$, which gave the above discrepancy. This prompted them to explore the possibility of including additional orbital decay mechanisms, such as dynamical friction caused by a dark matter density spike surrounding the primary SMBH, to explain the abovementioned discrepancy.

A few comments are needed before we delve into the $\dot{E}_{\rm GW} - \dot{E}$ consistency test of M. H. Chan & C. M. Lee (2024). First, it is critical to emphasize that the above test works if and only if the parameters used to evaluate Equations (1) and (3) are independently measured quantities. It turns out that this test, in principle, is similar to the way binary pulsars like PSR B1913+16 are employed to test GR in strong field regimes (I. H. Stairs 2003). In the case of binary pulsars, one measures the rate of change of orbital period $\dot{P}_b$ from the detailed analysis of decades-long ToAs from the constituent pulsar and checks its consistency with the GR prediction for $\dot{P}_b$ that requires independent measurements for the masses of the pulsar and its companion, orbital eccentricity, and orbital period. Therefore, performing a similar $\dot{E}_{\rm GW} - \dot{E}$ consistency test for PSR B1913 +16, the most celebrated pulsar binary (J. H. Taylor 1994), would be highly instructive. In contrast, a closer inspection of Table 2 of L. Dey et al. (2018) reveals that it contains OJ 287's measured and estimated parameters categorized as "independent" and "derived" quantities, respectively. Unfortunately, M. H. Chan & C. M. Lee (2024) did not differentiate between these two types of parameters while employing them to perform the above consistency test for the SMBH binary in OJ 287. An additional point is that L. Dey et al. (2018) did not provide any direct measurement of a, OJ 287's semimajor axis. Therefore, M. H. Chan & C. M. Lee (2024) relied on Kepler's third law, i.e., $P_b \propto a^{3/2}$ and incorporated derived values of a from M. J. Valtonen & H. J. Lehto (1997). In our opinion, it is not necessary to invoke semimajor axis a, especially when we have estimates for a gauge invariant quantity like P_b (T. Damour & G. Schafer 1988). This is another reason to take a closer look at their consistency test for OJ 287.

To clarify that the $\dot{E}_{\rm GW} - \dot{E}$ consistency test works if and only if the employed parameters are independently measured, we consider the observations of the first relativistic binary pulsar PSR B1913+16 (R. A. Hulse & J. H. Taylor 1975). By analyzing 9257 precise TOAs collected over 35 yr using the Arecibo Observatory, J. M. Weisberg & Y. Huang (2016) showed that the observed orbital period decay for PSR B1913 +16 closely matched with the associated GR prediction, with a discrepancy of less than $\sim 1\sigma$. To ensure that we employ only the measured parameters that arise from the many decades-long precise timing observations of PSR B1913+16, it is imperative to use the following quadrupolar-order expression for $\dot{E}_{\rm GW}$, extracted from Equation (4.20) in L. Blanchet & G. Schaefer (1989):

$$\dot{E}_{\rm GW} = -\frac{32}{5}\frac{\eta^2 (G\,M\,n/c^3)^{\frac{10}{3}}}{(1-e^2)^{\frac{7}{2}}}\left(1 + \frac{73}{24}e^2 + \frac{37}{96}e^4\right), \tag{4}$$

where $\eta = m_1 m_2/(m_1 + m_2)^2$ is the symmetric mass ratio and $n = 2\,\pi/P_b$ is the gauge invariant mean motion in s^{-1}. We have used $T_\odot = G M_\odot/c^3 = 4.925,\ 490,\ 947\ \mu$s while evaluating $(G\,M\,n/c^3)$, where $M_\odot$ stands for the solar mass. Additionally, we have scaled the above expression by c^5/G to deal with only a dimensionless expression, and this also takes care of the fact that G is a poorly measured quantity (C. Xue et al. 2020). We now express the time derivative of the orbital (binding) energy, given by Equation (3), in terms of the orbital period P_b and its time derivative $\dot{P}_b$, and it reads

$$\dot{E} = \frac{\eta (G\,M\,n/c^3)^{\frac{5}{3}} \dot{P}_b}{6\pi}. \tag{5}$$

This expression is also scaled by c^5/G so that we deal only with dimensionless expressions.

We now have all the inputs to pursue the $\dot{E}_{\rm GW} - \dot{E}$ consistency test with the help of independently measured parameters of an inspiraling compact binary. For pursuing the consistency test, we evaluate Equation (4) using the measured values of $P_b = 0.322997448918(3)$ days, $e = 0.6171340(4)$, $m_1 = 1.438 \pm 0.001 M_\odot$, and $m_2 = 1.390 \pm 0.001 M_\odot$, available in Table 2 of J. M. Weisberg & Y. Huang (2016). This results in the dimensionless $\dot{E}_{\rm GW} = -(2.14009 \pm 0.00357) \times 10^{-28}$ estimate for PSR B1913+16. We would like to emphasize that the above-measured values for the binary pulsar's orbital elements and parameters arise from the precise modeling of various relativistic effects that influence the ToAs of PSR B1913+16's radio pulses (J. M. Weisberg & Y. Huang 2016). These delays include the Roemer delay, caused by the motion of the pulsar in its orbit; the Shapiro delay, resulting from the curvature of spacetime near the companion star; and the Einstein delay, which accounts for gravitational time dilation and the pulsar's varying orbital velocity while incorporating post-Keplerian effects like the advance of periastron (J. M. Weisberg & Y. Huang 2016; I. H. Stairs 2003).

We now calculate the dimensionless value of $\dot{E}$ using Equation (5). Employing $\dot{P}_b = -(2.398 \pm 0.004) \times 10^{-12}$ for PSR B1913+16, as obtained through Equation (15) of J. M. Weisberg & Y. Huang (2016), the resulting expression evaluates to $-(2.13643 \pm 0.00398) \times 10^{-28}$. A close inspection of these two estimates reveals that the $\dot{E}_{\rm GW} - \dot{E}$ consistency test works for PSR B1913+16. It is important to note that the parameter $\dot{P}_b$ enters as an independent parameter in the Kepler equation, expressed in terms of proper time coordinates, in the heavily used Damour–Deruelle timing model (T. Damour & N. Deruelle 1986; I. H. Stairs 2003) and it reads

$$u - e \sin u = 2\pi \left\{ \frac{(t - t_0)}{P_b} - \frac{\dot{P}_b}{2} \left(\frac{(t - t_0)}{P_b} \right)^2 \right\}, \qquad (6)$$

where u is the eccentric anomaly and t_0 is the reference time for periastron passage. The use of the Damour–Deruelle timing formula ensures that the long-term timing of relativistic binary pulsars regularly leads to independently measured values for P_b, $\dot{P}_b$, and e along with the masses m_1 and m_2 (I. H. Stairs 2003; T. Damour & J. H. Taylor 1992). Influenced by J. M. Weisberg & Y. Huang (2016), we take the ratio of $\dot{E}_{\rm GW}$ and $\dot{E}$ for the binary pulsar, and we get its value to be 0.9983 ± 0.0025, which quantifies the consistency test of M. H. Chan & C. M. Lee (2024) for PSR B1913+16.

A few comments are in order. In the case of binary pulsars, it is customary to obtain estimates for the quadrupolar-order $\dot{P}_b$ expression, given by Equation (22) in J. M. Weisberg & Y. Huang (2016) and compare it with the measured intrinsic $\dot{P}_b$ values, given by Equation (15) in J. M. Weisberg & Y. Huang (2016). For PSR B1913+16, the ratio between $\dot{P}_b^{\rm intr}$ and $\dot{P}_b^{\rm GR}$ turned out to be 0.9983 ± 0.0016 as is evident from Equation (23) in J. M. Weisberg & Y. Huang (2016). This result implies that the binary pulsar is losing energy to GWs within $\sim 1\sigma$ of the rate predicted by GR. This is essentially the reason why the long-term timing of PSR B1913+16 provided the first indirect evidence for the existence of GWs (J. H. Taylor 1994). In contrast, the $\dot{E}_{\rm GW} - \dot{E}$ consistency test, as demonstrated by M. H. Chan & C. M. Lee (2024), is rather convoluted from the PSR B1913+16 perspective. This is because it requires us to employ P_b, $\dot{P}_b$, m_1, m_2, and e values while evaluating both the expressions and thereby mixing measured quantities that arise from the conservative and dissipative aspects of PN-accurate orbital dynamics of the compact binary present in PSR B1913+16 (T. Damour & J. H. Taylor 1992).

It should be obvious from these discussions that independent measurements of orbital elements and parameters are critical for performing the $\dot{E}_{\rm GW} - \dot{E}$ consistency test. In contrast to relativistic binary pulsars, both P_b and $\dot{P}_b$ are not observationally measurable quantities in our SMBH binary description for OJ 287 (L. Dey et al. 2018). This is mainly because we only have observational data for two epochs per orbit that are associated with secondary SMBH crossings for determining various astrophysical and relativistic aspects of OJ 287's SMBH binary, listed as "independent" parameters in Table 2 of L. Dey et al. (2018). Further, a pair of these epochs are not separated by exactly one orbital period due to substantial relativistic precession. These considerations prompted some of us to provide rough estimates for both the orbital period and its time derivative using the complete orbit solution/trajectory, and they were displayed as "derived" estimates in Table 2 of L. Dey et al. (2018). These rough estimates were displayed essentially to show the highly relativistic nature of OJ 287's SMBH binary compared to relativistic binary pulsars. In Table 2 of L. Dey et al. (2018), we extracted the orbital period value from the difference in two subsequent epochs of secondary SMBH apastron passages, namely, between 2013 and 2025 apocenter times. The epochs of apastron passages rather than pericenter passages were chosen due to the comparatively lower speed of the secondary at these epochs which allowed dense sampling of the trajectory numerically. After that, we estimated $\dot{P}_b$ using the differences in the P_b values between 1901 and 2021 and dividing them by the elapsed time of 120 yr. We would like to emphasize that these derived quantities played no role in the prediction of the 2019 impact flare though their accuracies are influenced by the orbital trajectory constructed with the help of Table 2 of L. Dey et al. (2018).

It is indeed possible to obtain accurate estimates for P_b and its time derivative using the "independent" parameters in Table 2 of L. Dey et al. (2018) with the help of the following steps. First, we compute the P_b estimate in the rest frame of the SMBH binary by employing the $\Delta\Phi = 2\pi k$ relation, where $\Delta\Phi$ represents the precession rate of the major axis per period and k denotes the fractional rate of advance of the periastron, and we use the 3PN-accurate expression for k available in C. Königsdörffer & A. Gopakumar (2006; see also Equation (A1) in L. Dey et al. 2018). Using measured parameters from Table 2 in L. Dey et al. (2018), we calculate the nonredshifted orbital period as $P_b = 9.231 \pm 0.034$ yr. Including the redshift effect yields the orbital period as $P_{\rm obs} = 12.056 \pm 0.044$ yr, which is not very different from the listed value of $P_{\rm orb}^{2017} = 12.062 \pm 0.007$ yr in L. Dey et al. (2018). For obtaining an accurate estimate for $\dot{P}_b$, we invoke Equation (2.8) from L. Blanchet & G. Schaefer (1989) and the relevant measured parameters in Table 2 of L. Dey et al. (2018), and it leads to $\dot{P}_b = -(0.000515 \pm 0.000006)$. We are now in a position to perform the $\dot{E}_{\rm GW} - \dot{E}$ consistency test. Substituting the above-derived values into Equations (4) and (5), we obtain $\dot{E}_{\rm GW} = -(6.782 \pm 0.111) \times 10^{-12}$ and $\dot{E} = -(6.782 \pm 0.520) \times 10^{-12}$ in dimensionless units. It should be obvious that there is no statistically significant difference between $\dot{E}_{\rm GW}$ and $\dot{E}$ as their central values are essentially identical. These results confirm that the $\dot{E}_{\rm GW} - \dot{E}$ consistency test holds well for OJ 287, provided we employ only the measured ("independent") parameters associated with its SMBH binary central engine description. The use of general relativistic inputs and observationally measured parameters of OJ 287, based on its SMBH binary central engine description, in the above consistency test shows that the orbital dynamics of SMBH binary in OJ 287 accurately follow general relativity. We want to note in passing that it is customary to use the dominant PN contribution to k for constraining the total mass of binary pulsars while the quadrupolar-order $\dot{P}_b$ expression is employed to estimate the expected rate of orbital decay in newly discovered binary pulsars (E. D. Barr et al. 2024).

To validate our abovementioned quadrupolar-order approach, we conducted a 1PN-accurate $\dot{E}_{\rm GW} - \dot{E}$ consistency test using expressions from L. Blanchet & G. Schaefer (1989), yielding $\dot{P}_b = -(0.000684 \pm 0.000009)$. This analysis revealed a good agreement between 1PN-accurate $\dot{E}_{\rm GW}$ and $\dot{E}$ estimates, with a discrepancy of only $\sim 0.41\sigma$. Specifically, the 1PN-accurate forms of Equations (4) and (5) give

$\dot{E}_{\rm GW} = -(9.268 \pm 0.161) \times 10^{-12}$ and $\dot{E} = -(9.355 \pm 0.136) \times 10^{-12}$, respectively. We pursued the above computations as the orbital dynamics of OJ 287 employ PN-accurate equations of motion that incorporated GW emission effects beyond the quadrupolar order (L. Dey et al. 2018). It is worthwhile to note that an additional subtlety was not addressed in (M. H. Chan & C. M. Lee 2024). It is desirable to employ the nonredshifted orbital period in theoretical calculations for $\dot{E}$ and $\dot{E}_{\rm GW}$ as these quantities are usually provided in the rest frame of a compact binary system. However, M. H. Chan & C. M. Lee (2024) used the redshifted $P_{\rm orb}^{2017}$ and the corresponding $\dot{P}_{\rm orb}$, as listed in Table 2 of L. Dey et al. (2018), in their the $\dot{E}_{\rm GW} - \dot{E}$ consistency test and their reported 4.3σ discrepancy. Interestingly, our quadrupolar and 1PN-accurate consistency tests required us to use the nonredshifted orbital period. These considerations suggest that the reported evidence for a dark matter density spike around the primary SMBH in OJ 287 and the derived spike index $\gamma_{\rm sp}$ require further scrutiny and revision. In what follows, we provide certain upper bounds for $\gamma_{\rm sp}$, derived under the revised framework.

3. Constraining $\gamma_{\rm sp}$ Using Timing Uncertainties in OJ 287's Impact Flare Observations

Our approach to constrain $\gamma_{\rm sp}$ is influenced by an effort by M. W. Horbatsch & C. P. Burgess (2012), who constrained the instantaneous time variation of "sufficiently light" scalar fields using inputs from OJ 287's SMBH binary description. This effort relies on an earlier result that showed that a BH should acquire "scalar hair," provided the underlying scalar field is slowly time dependent far from the BH (T. Jacobson 1999). Invoking the above result, it was argued that an orbiting pair of BHs can radiate dipole radiation, provided the two BHs have different masses (M. W. Horbatsch & C. P. Burgess 2012). Additionally, M. W. Horbatsch & C. P. Burgess (2012) computed an appropriate formula for the emitted power from the time-varying dipole moment, induced by the time-dependent scalar hair that resides on the constituent BHs in an inspiraling BH binary. It turns out that the ratio of dipolar to quadrupolar GW luminosities essentially depends on the frequency μ', which characterizes the variation of the scalar field far from the black hole binary and it requires good estimates for various orbital elements and parameters like m_1, m_2, e, and P_b (M. W. Horbatsch & C. P. Burgess 2012). This prompted M. W. Horbatsch & C. P. Burgess (2012) to equate the above ratio, computed for OJ 287's SMBH binary description as given in M. J. Valtonen et al. (2008), to <0.06. This fraction, as expected, essentially quantifies the uncertainty in predicting the arrival time of the observed 2007 impact flare while using 2.5PN-accurate orbital dynamics of nonspinning SMBH binaries (M. J. Valtonen et al. 2008). The resulting upper bound on the time variation of scalar fields turned out to be $<(16\ \text{days})^{-1}$. In what follows, we adopt a similar approach to constrain $\gamma_{\rm sp}$.

Recall that M. H. Chan & C. M. Lee (2024) introduced an additional mechanism involving energy dissipation through dynamical friction caused by a dark matter density spike surrounding the primary SMBH in OJ 287. This was, as noted earlier, influenced by their contestable inference that OJ 287's SMBH binary central engine description is inconsistent with their $\dot{E}_{\rm GW} - \dot{E}$ consistency test. To model the dark matter density near the primary SMBH, M. H. Chan & C. M. Lee (2024) employed the following spike profile:

$$\rho_{\rm DM} = \begin{cases} 0 & \text{for } r \leqslant 2R_s, \\ \rho_{\rm sp}\left(1 - \frac{2R_s}{r}\right)^3 \left(\frac{r}{r_{\rm sp}}\right)^{-\gamma_{\rm sp}} & \text{for } 2R_s < r \leqslant r_{\rm sp}, \\ \frac{\rho_s r_s}{r} & \text{for } r_{\rm sp} < r \ll r_s, \end{cases} \tag{7}$$

where r_s and ρ_S represent the scale radius and scale density, respectively, while the term $R_s = 2Gm_1/c^2$ stands for the Schwarzschild radius while $r_{\rm sp}$ is the radius of spike region and $\gamma_{\rm sp}$ is the spike index characterizing the DM density gradient within the spike region. The resulting orbital averaged energy-loss rate due to dynamical friction induced by the DM density spike surrounding the central SMBH reads (X.-J. Yue & Z. Cao 2019)

$$\dot{E}_{\rm DF} = -2G^{\frac{3}{2}}\mu^2\rho_{\rm sp}r_{\rm sp}^{\gamma_{\rm sp}}(1-e^2)^{\frac{3}{2}}\ln\Lambda \int_0^{2\pi} \times \frac{[1+e\cos(1-\alpha)\phi]^{\gamma_{\rm sp}-2}[p-2R_s(1+e\cos(1-\alpha)\phi)]^3}{p^{\gamma_{\rm sp}+\frac{5}{2}}m_1^{\frac{1}{2}}[1+2e\cos(1-\alpha)\phi+e^2]^{\frac{1}{2}}} d\phi, \tag{8}$$

where $\ln\Lambda \approx \ln\sqrt{m_1/m_2}$ is the Coulomb logarithm, p is the semi-latus rectum, α denotes the precession phase angle, and ϕ is the orbital phase. If the dark matter density is extremely high near the primary SMBH, dynamical friction could substantially alter the inspiral dynamics of OJ 287's SMBH binary. Therefore, M. H. Chan & C. M. Lee (2024) argued that the above contribution should be added to $\dot{E}_{\rm GW}$ while performing the above consistency test for OJ 287. In other words, M. H. Chan & C. M. Lee (2024) argued that it was the neglect of the $\dot{E}_{\rm DF}$ contribution that caused the failure of the $\dot{E}_{\rm GW} - \dot{E}$ consistency test for OJ 287 while using the measured and estimated parameters listed in Table 2 of L. Dey et al. (2018). This prompted M. H. Chan & C. M. Lee (2024) to equate $\dot{E}_{\rm GW} + \dot{E}_{\rm DF}$, given by Equations (4) and (8) to the $\dot{E}$ expression, given by Equation 3, while using various parameters listed in Table 2 of L. Dey et al. (2018) and a value of a as obtained by M. J. Valtonen & H. J. Lehto (1997). This resulted in Figure 1 of M. H. Chan & C. M. Lee (2024), and it should be obvious that they were able to estimate accurately a value for the dark matter density spike $\gamma_{\rm sp} = 2.351^{+0.032}_{-0.045}$. It turned out that this value aligns closely with the canonical model prediction of $\gamma_{\rm sp} = 2.333$ (P. Gondolo & J. Silk 1999; T. Lacroix 2018). In our opinion, this estimate requires further scrutiny due to our way of showing the $\dot{E}_{\rm GW} - \dot{E}$ consistency for OJ 287 as discussed in Section 2.

Our approach to constrain $\gamma_{\rm sp}$, as noted earlier, is influenced by M. W. Horbatsch & C. P. Burgess (2012), and therefore it involves first computing the ratio $\dot{E}_{\rm DF}/\dot{E}_{\rm GW}$, given by Equations (4) and (8). Thereafter, we equate the ratio to the uncertainties in our ability to predict the observed 2015 and 2019 impact flares from OJ 287. The 2019 outburst, originating near the disk's pericenter, turned out to be fairly identical to the 2007 outburst in our SMBH binary central engine description for OJ 287 (L. Dey et al. 2018). The eventual observation of the 2019 outburst with a light curve similar to the one associated with the 2007 impact flare allowed us to provide consistency in our observations with its GR prediction to within 1% (S. Laine

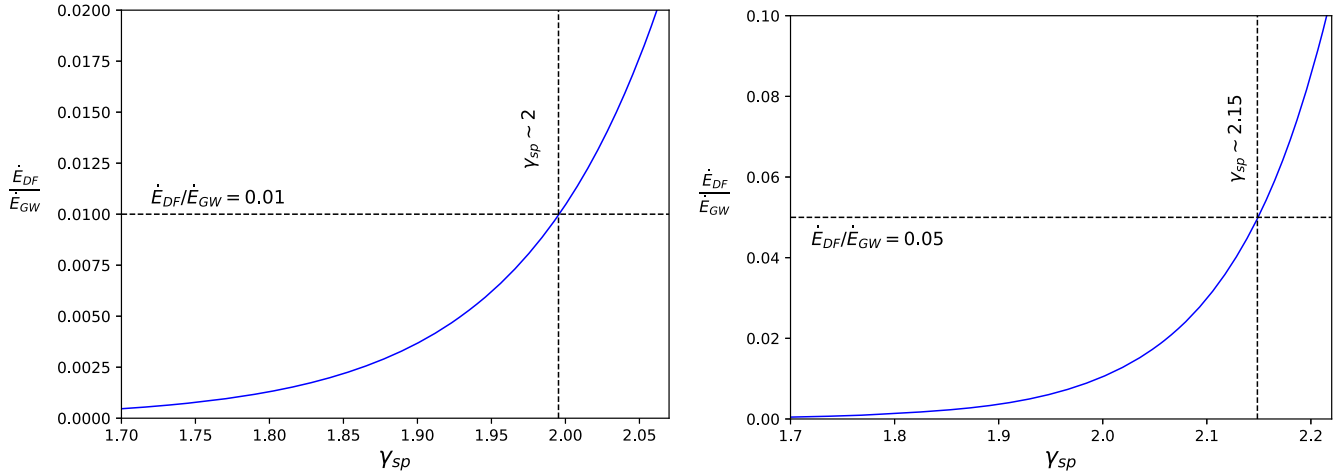

Figure 1. Plots for the variation of the ratio $\dot{E}_{\rm DF}/\dot{E}_{\rm GW}$ as a function of $\gamma_{\rm sp}$ while using SMBH binary description of OJ 287 as given in Table 2 of L. Dey et al. (2018). The uncertainty levels associated with the observed 2015 and 2019 impact flares in our model lead to upper bounds marked by the dashed lines, influenced by the approach of M. W. Horbatsch & C. P. Burgess (2012). Both these upper bounds are inconsistent with the estimated value of $\gamma_{\rm sp}$ by M. H. Chan & C. M. Lee (2024).

et al. 2020). In contrast, the 2015 flare, originating closer to the apocenter with timing consistency within 5% of GR predictions (M. J. Valtonen et al. 2016). Therefore, we let the above ratio be 1% and 5% to obtain upper bounds on $\gamma_{\rm sp}$. We obtain an upper bound of $\gamma_{\rm sp}$ as $\sim$2 and 2.15 for uncertainties of 1% and 5%, respectively, by invoking the ratio $\dot{E}_{\rm DF}/\dot{E}_{\rm GW}$. In other words, we argue that uncertainties in predicting the observed impact flares may be associated with OJ 287's orbital damping induced by dynamical friction associated with a dark matter density spike around its primary SMBH. Additionally, we used the nonredshifted P_b instead of the semimajor axis to compute $\dot{E}_{\rm DF}$, as given by Equation (8). The results are presented in Figure 1. It should be obvious that it is not possible for us to estimate an accurate value for $\gamma_{\rm sp}$ but to provide only interesting upper bounds. This is not surprising as we do not follow the arguments of M. H. Chan & C. M. Lee (2024) that the $\dot{E}_{\rm GW}$ value needs to be supplemented by the $\dot{E}_{\rm DF}$ contribution to account for their inferred value for $\dot{E}$. Moreover, since the $\dot{E}_{\rm GW} - \dot{E}$ consistency test performs well for SMBH binary systems like OJ 287, it supports the presence of "sufficiently light" scalar fields around OJ 287, as argued by M. W. Horbatsch & C. P. Burgess (2012). This method provides a plausible approach to constrain the upper bound of $\gamma_{\rm sp}$ using the ratio $\dot{E}_{\rm DF}/\dot{E}_{\rm GW}$ while accounting for the uncertainties in predicting the observed impact flares of OJ 287.

4. Conclusions and Discussions

We provide a way to pursue the $\dot{E}_{\rm GW} - \dot{E}$ consistency test for OJ 287, proposed by M. H. Chan & C. M. Lee (2024), while employing independently measured parameters from Table 2 of L. Dey et al. (2018) for describing OJ 287's SMBH binary central engine. This prompted us to probe the reported evidence for a dark matter density spike around the primary SMBH in OJ 287 and their way of estimating the spike index $\gamma_{\rm sp}$. After that, we provided upper bounds for $\gamma_{\rm sp}$ by employing the uncertainties in the observed 2015 and 2019 impact flares to their GR-based predictions, influenced by M. W. Horbatsch & C. P. Burgess (2012). The resulting upper bounds $\gamma_{\rm sp}$ turned out to be $\sim$2 and 2.15 when we let the ratio $\dot{E}_{\rm DF}/\dot{E}_{\rm GW}$ be 0.01 and 0.05, respectively.

The above upper bounds may have implications for a recent interesting effort that placed an upper bound on the DM spike mass surrounding the primary SMBH of OJ 287 (A. Alachkar et al. 2023). This detailed analysis puts the above mass to be less than 3% of the mass of the primary SMBH, assuming $\gamma_{\rm sp} \sim 2.333$ (T. Lacroix 2018). Additionally, it would be worthwhile to explore how these upper bounds on $\gamma_{\rm sp}$ influence the constraints on the dark matter spike mass around the primary SMBH in OJ 287, as discussed in A. Alachkar et al. (2023), potentially advancing our understanding of DM profiles in such systems.

Acknowledgments

We thank Gonzalo Alonso Alvarez for helpful discussions and suggestions. D.D. acknowledges the Department of Atomic Energy, Government of India's support through "Apex Project-Advance Research and Education in Mathematical Sciences" at The Institute of Mathematical Sciences. A.G. acknowledges the support of the Department of Atomic Energy, Government of India, under project identification #RTI4002. We sincerely thank the anonymous referee for the insightful comments and valuable suggestions.

ORCID iDs

Debabrata Deb https://orcid.org/0000-0003-4067-5283
Achamveedu Gopakumar https://orcid.org/0000-0003-4274-4369
Mauri J. Valtonen https://orcid.org/0000-0001-8580-8874

References

Afzal, A., Agazie, G., Anumarlapudi, A., et al. 2023, ApJL, 951, L11
Agazie, G., Antoniadis, J., Anumarlapudi, A., et al. 2024, ApJ, 966, 105
Agazie, G., Anumarlapudi, A., Archibald, A. M., et al. 2023a, ApJL, 952, L37
Agazie, G., Anumarlapudi, A., Archibald, A. M., et al. 2023b, ApJL, 951, L8
Agazie, G., Anumarlapudi, A., Archibald, A. M., et al. 2023c, ApJL, 951, L50
Alachkar, A., Ellis, J., & Fairbairn, M. 2023, PhRvD, 107, 103033
Armitage, P. J., & Natarajan, P. 2002, ApJL, 567, L9
Barr, E. D., Dutta, A., Freire, P. C. C., et al. 2024, Sci, 383, 275
Baugh, C. M. 2006, RPPh, 69, 3101
Begelman, M. C., Blandford, R. D., & Rees, M. J. 1980, Natur, 287, 307
Blanchet, L. 2024, LRR, 27, 4
Blanchet, L., & Schaefer, G. 1989, MNRAS, 239, 845
Chan, M. H., & Lee, C. M. 2024, ApJL, 962, L40

Damour, T., & Deruelle, N. 1986, AIHPA, 44, 263
Damour, T., & Schafer, G. 1988, NCimB, 101B, 127
Damour, T., & Taylor, J. H. 1992, PhRvD, 45, 1840
Desvignes, G., Caballero, R. N., Lentati, L., et al. 2016, MNRAS, 458, 3341
Dey, L., Gopakumar, A., Valtonen, M., et al. 2019, Univ, 5, 108
Dey, L., Valtonen, M. J., Gopakumar, A., et al. 2018, ApJ, 866, 11
EPTA Collaboration, Antoniadis, J., Babak, S., et al. 2023a, A&A, 678, A48
EPTA Collaboration InPTA Collaboration, Antoniadis, J., et al. 2024a, A&A, 685, A94
EPTA Collaboration InPTA Collaboration, Antoniadis, J., et al. 2023b, A&A, 678, A50
EPTA Collaboration InPTA Collaboration, Antoniadis, J., et al. 2024b, A&A, 690, A118
Falxa, M., Babak, S., Baker, P. T., et al. 2023, MNRAS, 521, 5077
Fields, B. D., Shapiro, S. L., & Shelton, J. 2014, PhRvL, 113, 151302
Gondolo, P., & Silk, J. 1999, PhRvL, 83, 1719
Hallinan, G., Ravi, V., Weinreb, S., et al. 2019, BAAS, 51, 255
Horbatsch, M. W., & Burgess, C. P. 2012, JCAP, 2012, 010
Hulse, R. A., & Taylor, J. H. 1975, ApJL, 195, L51
Königsdörffer, C., & Gopakumar, A. 2006, PhRvD, 73, 124012
Iwasawa, M., An, S., Matsubayashi, T., et al. 2011, ApJL, 731, L9
Jacobson, T. 1999, PhRvL, 83, 2699
Joshi, B. C., Arumugasamy, A., Bagchi, M., et al. 2018, JApA, 39, 51
Joshi, B. C., Gopakumar, A., Pandian, A., et al. 2022, JApA, 43, 98
Kulkarni, G., & Loeb, A. 2012, MNRAS, 422, 1306
Lacroix, T. 2018, A&A, 619, A46
Laine, S., Dey, L., Valtonen, M., et al. 2020, ApJL, 894, L1
Lehto, H. J., & Valtonen, M. J. 1996, ApJ, 460, 207
Liao, S., Irodotou, D., Johansson, P. H., et al. 2024, MNRAS, 528, 5080
Liu, T., Cohen, T., McGrath, C., et al. 2023, ApJ, 945, 78
Manchester, R. N., Hobbs, G., Bailes, M., et al. 2013, PASA, 30, e017
Miles, M. T., Shannon, R. M., Bailes, M., et al. 2023, MNRAS, 519, 3976
O'Neill, S., Kiehlmann, S., Readhead, A. C. S., et al. 2022, ApJL, 926, L35
Padmanabhan, H., & Loeb, A. 2023, A&A, 676, A115
Reardon, D. J., Zic, A., Shannon, R. M., et al. 2023, ApJL, 951, L6
Stairs, I. H. 2003, LRR, 6, 5
Tarafdar, P., Nobleson, K., Rana, P., et al. 2022, PASA, 39, e053
Taylor, J. H., Jr. 1994, RvMP, 66, 711
Valtonen, M., & Karttunen, H. 2006, The Three-Body Problem (Cambridge: Cambridge Univ. Press), 2006
Valtonen, M. J., Dey, L., Gopakumar, A., et al. 2021, Galax, 10, 1
Valtonen, M. J., Dey, L., Hudec, R., et al. 2018, in IAU Symp. 338, Gravitational Wave Astrophysics: Early Results from Gravitational Wave Searches and Electromagnetic Counterparts (Cambridge: Cambridge Univ. Press), 29
Valtonen, M. J., & Lehto, H. J. 1997, ApJL, 481, L5
Valtonen, M. J., Lehto, H. J., Nilsson, K., et al. 2008, Natur, 452, 851
Valtonen, M. J., Nilsson, K., Sillanpää, A., et al. 2006, ApJL, 643, L9
Valtonen, M. J., Zola, S., Ciprini, S., et al. 2016, ApJL, 819, L37
Valtonen, M. J., Zola, S., Gupta, A. C., et al. 2024, ApJL, 968, L17
Wang, Y., & Mohanty, S. D. 2017, PhRvL, 118, 151104
Weisberg, J. M., & Huang, Y. 2016, ApJ, 829, 55
Xu, H., Chen, S., Guo, Y., et al. 2023, RAA, 23, 075024
Xue, C., Liu, J. P., Li, Q., et al. 2020, NSRev, 7, 1803
Yue, X.-J., & Cao, Z. 2019, PhRvD, 100, 043013
Zic, A., Reardon, D. J., Kapur, A., et al. 2023, PASA, 40, e049